Molecular Cancer Therapeutics

Ormeloxifene Suppresses Prostate Tumor Growth and Metastatic Phenotypes via Inhibition of Oncogenic β-catenin Signaling and EMT Progression

Bilal Bin Hafeez[1], Aditya Ganju[1], Mohammed Sikander[1], Vivek K. Kashyap[1], Zubair Bin Hafeez[2], Neeraj Chauhan[1], Shabnam Malik[1], Andrew E. Massey[1], Manish K. Tripathi[1], Fathi T. Halaweish[3], Nadeem Zafar[4], Man M. Singh[5], Murali M. Yallapu[1], Subhash C. Chauhan[1], and Meena Jaggi[1]

Abstract

Ormeloxifene is a clinically approved selective estrogen receptor modulator, which has also shown excellent anticancer activity, thus it can be an ideal repurposing pharmacophore. Herein, we report therapeutic effects of ormeloxifene on prostate cancer and elucidate a novel molecular mechanism of its anticancer activity. Ormeloxifene treatment inhibited epithelial-to-mesenchymal transition (EMT) process as evident by repression of N-cadherin, Slug, Snail, vimentin, MMPs (MMP2 and MMP3), β-catenin/TCF-4 transcriptional activity, and induced the expression of pGSK3β. In molecular docking analysis, ormeloxifene showed proficient docking with β-catenin and GSK3β. In addition, ormeloxifene induced apoptosis, inhibited growth and metastatic potential of prostate cancer cells and arrested cell cycle in G_0–G_1 phase via modulation of cell-cycle regulatory proteins (inhibition of Mcl-1, cyclin D1, and CDK4 and induction of p21 and p27). In functional assays, ormeloxifene remarkably reduced tumorigenic, migratory, and invasive potential of prostate cancer cells. In addition, ormeloxifene treatment significantly ($P < 0.01$) regressed the prostate tumor growth in the xenograft mouse model while administered through intraperitoneal route (250 μg/mouse, three times a week). These molecular effects of ormeloxifene were also observed in excised tumor tissues as shown by immunohistochemistry analysis. Our results, for the first time, demonstrate repurposing potential of ormeloxifene as an anticancer drug for the treatment of advanced stage metastatic prostate cancer through a novel molecular mechanism involving β-catenin and EMT pathway. *Mol Cancer Ther; 16(10); 2267–80. ©2017 AACR.*

Introduction

Prostate cancer is the second leading cause of cancer-related death among American men. The American Cancer Society projected that a total of 161,360 new cases of prostate cancer would be diagnosed and approximately 26,730 men will die in the United States alone in the year of 2017 (1). Despite the initial success of androgen-ablation therapy, resistance to anti-androgen therapy manifests by progression to androgen-independent prostate cancer, which is the end stage that accounts for the majority of cancer deaths (2). Current chemotherapeutic drugs such as docetaxel, cabazitaxel, and mitoxantrone provide moderate treatment benefits for the management of advanced prostate cancer, but all of them suffer from severely toxic side effects. Moreover, these drugs do not target major oncogenic signaling pathways such as β-catenin/epithelial-to-mesenchymal transition (EMT), which lead to tumor growth and metastasis of prostate cancer (3).

Studies have shown that loss of E-cadherin and overexpression of N-cadherin is involved in EMT, leading to aggressive and metastatic prostate cancer phenotypes (4, 5). Altered β-catenin expression/subcellular localization also plays a major role in EMT process in various malignancies including prostate cancer (6). Studies have suggested involvement of β-catenin in the development, progression, and therapy resistance of advanced prostate cancer (3). β-catenin is present in the cytoplasm as a heterodimeric protein complex that includes glycogen synthase kinase 3β (GSK3β), axin, and adenomatosis polyposis coli (APC; ref. 7). GSK3β-dependent phosphorylation of β-catenin enhances its proteasomal degradation and inhibits its translocation into the nucleus, where it binds to T-cell Factor (*Tcf*) family of transcription factors, leading to transcriptional activation of various downstream target oncogenes. Various studies including ours have reported increased nuclear β-catenin expression correlates with higher prostate tumor grades as compared with normal adjacent tissues (5, 8). The stabilization of the transcriptional co-activator

[1]Department of Pharmaceutical Sciences, University of Tennessee Health Science Centre, Memphis, Tennessee. [2]Department of Biosciences, Jamia Millia Islamia, New Delhi, Delhi, India. [3]South Dakota State University, Brookings, South Dakota. [4]Department of Pathology, University of Tennessee Health Science Center, Memphis, Tennessee. [5]Saraswati Dental College, Lucknow, Uttar Pradesh, India.

Note: Supplementary data for this article are available at Molecular Cancer Therapeutics Online (http://mct.aacrjournals.org/).

B.B. Hafeez, A. Ganju, and M. Sikander contributed equally to this article.

Corresponding Authors: Subhash C. Chauhan, University of Tennessee Health Science Center, 19S Manassas Avenue, Memphis, TN 38163. Phone: 901-448-2175; Fax: 901-448-1051; E-mail: schauha1@uthsc.edu; and Meena Jaggi, mjaggi@uthsc.edu

doi: 10.1158/1535-7163.MCT-17-0157

β-catenin regulates expression of many genes which are involved in cell proliferation, differentiation, and the EMT (9). These studies suggest that β-catenin appears to be a very important molecular target in cancer therapy, and its targeting may lead to successful therapeutic approach for the management of metastatic prostate cancer. Thus, there is an urgent need to develop nontoxic agents/pharmacologic inhibitors that target aforementioned signaling pathways. These agent(s) could be used alone or in combination with conventional chemotherapy for the treatment of advanced prostate cancer.

Ormeloxifene has demonstrated excellent anticancer activity in many different tumor types such as breast cancer (10), head and neck squamous cell carcinoma (HNSCC; ref. 11), and ovarian cancer (12). We have recently demonstrated potent therapeutic efficacy of ormeloxifene in pancreatic cancer via inhibiting sonic hedgehog (SHH) signaling pathway, and modulation of tumor microenvironment (13). However, its effects on EMT processes and Wnt/β-catenin signaling are not investigated thus far. Herein, we have shown that ormeloxifene effectively inhibits molecular signatures of EMT, β-catenin/TCF-4 transcriptional activity, and induces phosphorylation of GSK3β, and degrades β-catenin leading to the suppression of prostate tumor growth in xenograft mouse model. Because ormeloxifene is reported to have an excellent therapeutic index and is safe for human use for antifertility (contraception) purpose (14), ormeloxifene appears to be an ideal pharmacologic agent for its repurposing as an anticancer agent against metastatic prostate cancer.

Materials and Methods

Cell lines

The human prostate cancer cells (PC3 and DU145) were the kind gift from Dr. Rajesh Singh, Assistant Professor, Morehouse School of Medicine, Atlanta, GA. They purchased these cells from ATCC in January, 2016. Upon receipt cells were expanded and frozen aliquots (passage < 6) were stored in liquid nitrogen. When needed, cells were thawed and grown for less than 6 months. These cell lines were propagated in RPMI1647 media supplemented with 10% FBS and 1× antibiotic and antimycotic solution. The media components were purchased from Lonza (Basel Switzerland).

Chemicals and antibodies

Specific monoclonal and polyclonal antibodies of β-actin (cat. no. 3700), cyclin D1 (cat. no. 2922), CDK4 (cat. no. 12790), p21 (cat. no. 2947), p27 (cat. no. 3686), Mcl-1 (cat. no. 5453), pGSK3β (cat. no. 5558), Histone H3 (cat. no. 4499), GAPDH (cat. no. 5174), N-cadherin (cat. no. 4061), Slug (cat. 9585), Snail (cat. no. 3879), Vimentin (cat. no. 5741), PARP (cat. no. 9532S), and MMP2 (cat. no. 4022) were obtained from Cell Signaling Technology Inc. β-catenin (cat. no. SC-7199), E-cadherin (cat. no. SC-7870), and MTA1 (cat. no. SC-17773) antibody was obtained from Santa Cruz Biotechnology. MMP3 (cat. no. IM36) antibody was procured from Calbiochem, Merck Biosciences. Horseradish peroxidase (HRP)-conjugated anti-mouse and anti-rabbit antibodies were acquired from Promega. Anti-mouse Cy3 secondary antibody was purchased from Thermo Fisher Scientific. Ormeloxifene was synthesized and characterized in Dr. Fathi Halaweish laboratory at South Dakota State University, Brookings, SD. The detail procedure for synthesis and characterization is described in our previous published manuscript (12).

MTT assay

Cell proliferation was determined by using MTT assay. Briefly, 5×10^3 cells of PC3 or DU145 were plated in 96-well plates and incubated for 24 hours in incubator at 37°C containing 5% CO_2. Cells were treated with ormeloxifene (5–40 μmol/L) for 24 and 48 hours. Twenty microliter of 5 mg/mL MTT was added in each well containing 100 μL of cell media. The cells were then further incubated for 6 hours in incubator and media was replaced with 150 μL of DMSO. Plates was vigorously shaked for 15 minutes and absorbance was taken at 570 nm on microplate reader (Cytation 3; BioTek).

Colony forming assay

To investigate the effects of ormeloxifene on clonogenic potential of PC3 and DU145 cells, colony formation assay was performed. In brief, 500 cells were seeded per well in six-well plate and allowed to stand for next 3 days. The cells were treated with ormeloxifene (2.5–7.5 μmol/L) for 7 days. Control cells were treated with DMSO (0.1%) as a vehicle control. The cells were maintained under standard cell culture conditions at 37°C and 5% CO_2 in a humid environment. Colonies were fixed in methanol, stained with hematoxylin, and counted using UVP 810 software.

Western blot analysis

Western blot analysis was performed to investigate the effect of ormeloxifene on protein levels of various oncogenes linked to prostate carcinogenesis. Briefly, prostate cancer cells (70–80% confluent) were treated with ormeloxifene (10–20 μmol/L) concentrations for 24 hours. Control cells were treated with vehicle (0.1% DMSO). Total cell lysates were prepared as described (15). Cytoplasmic and nuclear lysates were prepared using Nuclear Extract Kit (Active Motif). Forty microgram of protein lysates were subjected for Western blot analysis using 4% to 20% SDS-PAGE gels, blotted onto polyvinylidene difluoride (PVDF) membrane (Bio-Rad), and blocked with 10% BSA 1 hour at room temperature. The membranes were then incubated with the indicated primary antibodies followed by a HRP secondary antibody and developed with enhanced chemiluminescence reagent (Roche) using a UVP gel documentation system.

Immunofluorescence analysis

To determine the effect of ormeloxifene on β-catenin localization, 30,000 cells were seeded in four wells chamber slide. Next day, ormeloxifene (10 μmol/L) treatment was given for 24 hours. Localization of β-catenin was monitored by performing immunofluorescence analysis using confocal microscopy as described (16).

TCF luciferase assay

To investigate the effect of ormeloxifene on TCF promoter activity, we performed TCF luciferase assay. The reporter constructs were a generous gift from Dr. R. Moon (University of Washington, Seattle, WA). In this experiment, DU145 cells (1.5×10^5 cells/well) were plated in triplicate in 12-well plates. Cells were transiently co-transfected with TCF-firefly luciferase reporter constructs (pTOP-FLASH; 1 μg) and *Renilla* luciferase (200 ng) or (pFOP-FLASH; 1 μg) and *Renilla* luciferase (200 ng). After 24 hours, cells were treated with ormeloxifene (10 and 20 μmol/L) and lysates prepared at 6 hours posttreatment. Firefly and *Renilla* luciferase activity was analyzed by using Dual Luciferase Kit

(Promega). The β-catenin/TCF transcription activity was determined by normalizing the *Firefly* luciferase activity to that of *Renilla* luciferase activity and calculating the ratio of TOP-FLASH signal to FOP-FLASH signal.

Pulse chase assay

Pulse chase experiment was performed to determine the effect of ormeloxifene on β-catenin degradation using translational inhibitor cyclohexamide. Briefly, 70% confluent DU145 cells were treated with cyclohexamide (50 μg/mL) alone or in combination with ormeloxifene (15 μmol/L) for 1 to 24 hours. Cell lysates was prepared and protein levels of β-catenin was analyzed by Western blot analysis.

Molecular docking

Molecular docking experiments were conducted to know whether and where ormeloxifene binds in β-catenin (PDB ID: 4DJS; ref. 17) and GSK3β (PDB ID: 4ACH; ref. 18) proteins. The 2D and 3D structure of ormeloxifene were taken from (https://pubchem.ncbi.nlm.nih.gov/compound/154413#section=Top) Pub Chem. These experiments were performed using autodock 4.2 suit by employing Lamarckian genetic algorithm (19). The grid map illustrating the active site pocket for ligands were calculated by autogrid and the dimension of the grid for 4DJS and 4ACH were $56 \times 50 \times 90$ and $60 \times 62 \times 70$ grid points respectively with a spacing of 0.375 A° between the grid points and centered on the ligand. Docking was accomplished by each cycle with an initial population of 150 individuals and the remaining parameter set as default. Ten conformational docking poses were created and the best docked confirmation was selected based on the autodock binding energy (20). The confirmations with the most favorable free binding energy were selected for analyzing the interactions between the target receptor and ligands by visualization with Discovery Studio Software (version 3.5).

Chemoinvasion assay

Cell invasion assay was performed using a Cell Invasion Kit (BD Biocoat Matrigel Invasion Chambers; BD Biosciences). All procedures were followed as per the manufacturer's instructions. In brief, PC3 cells (50,000 cells/well) were seeded in an upper chamber containing serum free medium and further treated with ormeloxifene (5–15 μmol/L) or 0.1% DMSO as vehicle for 24 hours. The lower chamber was filled with 500 μL of media containing 20% FBS. Forty-eight hours posttreatment, cells were completely removed from inside the upper chamber by cotton swab. Cells were fixed with methanol and stained with Crystal Violet. Invaded cells were observed by using a light microscope at 100× magnification. Cells that had invaded the matrix membrane were counted in three random fields of view and the experiments were performed in triplicate.

Cell migration assay

Cell migration assay was performed using Boyden's Chambers (BD Biosciences), as per manufacturer's protocol. After 48 hours incubation, the migrating cells were fixed with methanol and stained with crystal violet and photographed under light microscope. Migratory cells in ormeloxifene-treated group were compared with control.

Cell proliferation, invasion, and migration by real-time xCELLigence system

To further confirm the functional impact of ormeloxifene on migration, invasion, and proliferation of prostate cancer cells, real-time proliferation, invasion, and migration assays were performed using the xCELLigence system as described (13). Briefly, 5×10^3 prostate cancer cells were seeded per chamber of cell proliferation or invasion and 7×10^4 cells/well for migration. After 24 hours, ormeloxifene (5–15 μmol/L) or the vehicle control (0.1% DMSO) was added and the experiment was allowed to run for 48 hours. Average baseline cell index of ormeloxifene-treated cells was calculated and compared with vehicle-treated control cells.

Agarose bead assay

Effect of ormeloxifene on cellular motility was determined by an agarose bead-based cell motility assay as described (21).

Cell-cycle analysis

In this experiment, approximately 70% confluent PC3 cells were synchronized by overnight starvation of cells in serum-free media. Cells were treated with ormeloxifene (10–20 μmol/L) for 24 hours and cell-cycle analysis was performed by flow cytometry as described (12).

Apoptosis analysis

Effect of ormeloxifene treatment on apoptosis induction in prostate cancer cells was analyzed using Annexin V-7AAD Apoptosis Kit (BD Biosciences) as described (15). In brief, PC3 and DU145 cells (200,000 cells per well) were plated in six-well plates and allowed to attach overnight. Next day, cells were treated with ormeloxifene (10–20 μmol/L) concentrations for 24 hours. Both floating and adherent cells were collected, washed twice with cold PBS, and stained with Annexin V-7AAD (5 μL) each/100 μL of cell suspension for 20 minutes in dark at room temperature. Number of apoptotic cells were analyzed by setting FL2 (Annexin V) and FL3 (7AAD) channels in BD Accuri flow cytometer (BD Biosciences). To analyze the effect of ormeloxifene on mitochondrial membrane potential ($\Delta\psi m$), we utilized tetramethyl rhodamine ethyl ester (TMRE) as described (12).

Xenograft study

A total of 12 athymic nude male mice were used to investigate the effect of ormeloxifene on PC3 cells derived xenograft tumors. The mice were maintained in a pathogen-free environment and all were carried out as per our approved protocol by the UTHSC Institutional Animal Care and Use Committee (IACUC). Briefly, PC3 cells (2×10^6) were dispersed in 100 μL 1:1 ratio of 1× PBS and 100 μL Matrigel (BD Biosciences) and injected subcutaneously into the dorsal flank of each mouse. The mice were periodically monitored for tumor development and the tumor volume was measured using a digital Vernier caliper. The tumor volume was calculated using the ellipsoid volume formula: tumor volume (mm^3) $= \pi/6 \times L \times W \times H$, wherein L is length, W is width, and H is height. The mice were given intraperitoneal injection of ormeloxifene (250 μg/mice) and 0.2% ethanol in PBS three times a week for 6 consecutive weeks starting from week 1st. The tumor volume was regularly monitored and allowed to grow until the tumor burden reached a maximum volume of 1,100 mm^3. At the time of sacrifice, the mice tumors were

removed, fixed in formalin, embedded in paraffin, and sliced into 5 μm sections for further biochemical analysis.

Immunofluorescence and immunohistochemistry analyses

Immunofluorescence analysis was performed to detect changes occur in the expression of β-catenin in excised xenograft tumor tissues of control and ormeloxifene-treated mice as described (21).

Statistical analysis

Statistical analysis was performed using an unpaired two-tailed Student t test and employed to assess the statistical significance between the control and ormeloxifene-treated groups. P value < 0.05 was considered as significant.

Results

Ormeloxifene treatment inhibits the growth of prostate cancer cells

Metastatic prostate cancer is the significant cause of mortality and morbidity in prostate cancer patients (22). Thus, we examined the anticancer effects of ormeloxifene on human prostate cancer cell lines (LNCaP, C4-2, PC3, and DU145) by cell counting assay (Supplementary Fig. S1). We performed additional cell proliferation assays (MTS assay and real-time xCELLigence assay) in two highly metastatic prostate cancer cell lines (PC3 and DU145). Ormeloxifene treatment inhibited viability of both PC3 and DU145 cells in a (10–40 μm) dose-dependent manner. The IC_{50} of ormeloxifene in PC3 and DU145 cells was 22 and 17 μmol/L, respectively (Fig. 1Ai–ii), after 24 hours treatment,

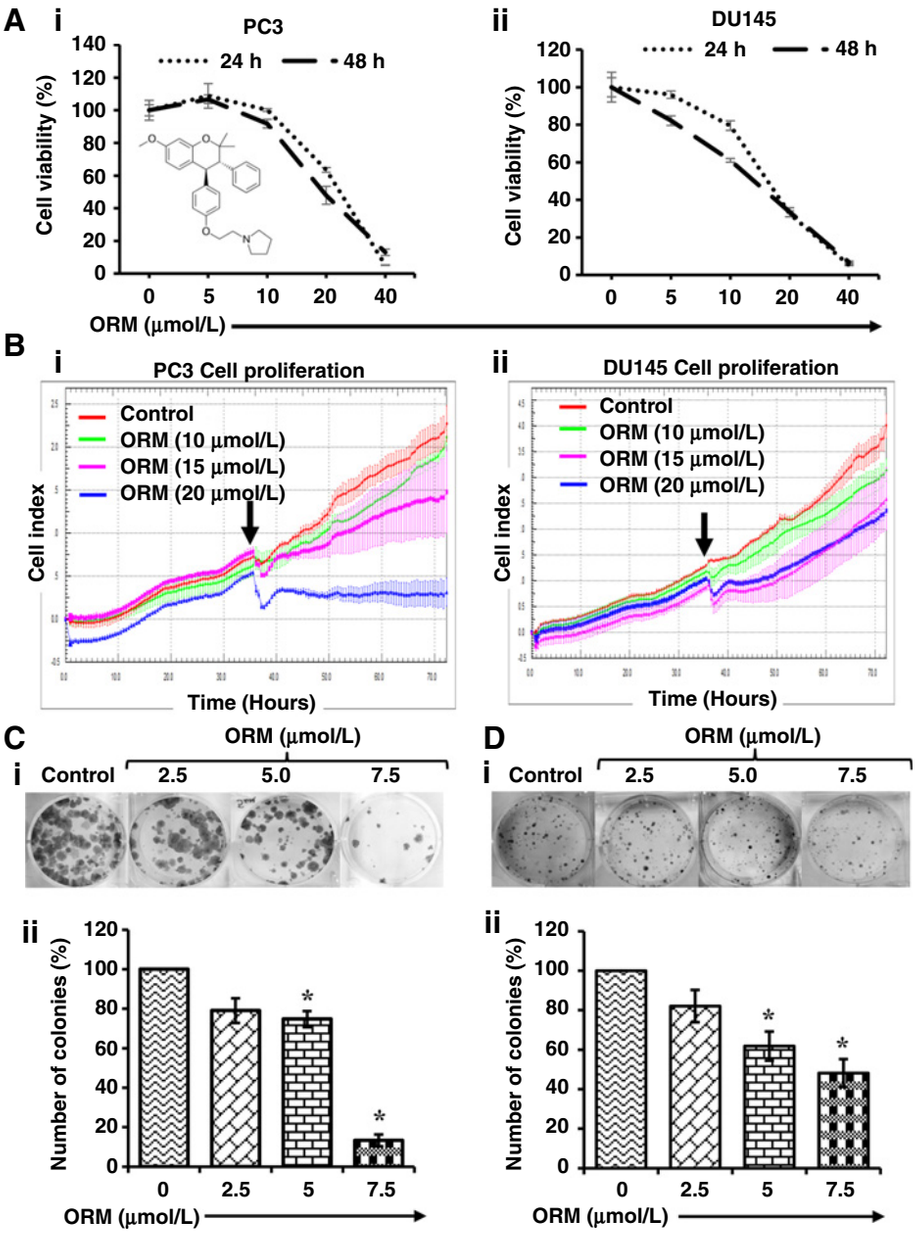

Figure 1.

Ormeloxifene (ORM) inhibits the growth of hormone refractory prostate cancer cells. **A**, Effect of ORM on cell viability of PC3 (i) and DU145 (ii) cells. Briefly, cells (2,500) were seeded in each well of 96-well plate and after overnight incubation, cells were treated with the indicated concentrations of ormeloxifene for 24 and 48 hours. Cell viability was assessed by MTT assay. The line graph represents the percent viable cells compared with the vehicle-treated group cells. Each concentration value is the mean ± SE of triplicate wells of each group. **B**, Effect of ormeloxifene on prostate cancer cells proliferation. Briefly, prostate cancer cells (5,000 cells/well) were seeded in E-plate (xCELLigence) following the xCELLigence Real-Time Cell Analyzer (RTCA) DP instrument manual as provided by the manufacturer. After 38 hours, ormeloxifene or the vehicle control was added and the experiment was allowed to run for 80 hours. Average baseline cell index for ormeloxifene-treated PC3 (**Bi**) and DU145 (**Bii**) cells was compared with vehicle-treated group. **C** and **D,** Effect of ormeloxifene on clonogenic potential of prostate cancer cells. Representative colony images of control and ormeloxifene-treated PC3 (**Ci**) and DU145 (**Di**) cells. Bar graphs indicating quantification of colony formation in PC3 (**Cii**) and DU145 (**Dii**) cells. Asterisk (*) denotes the significant value $P < 0.05$.

whereas IC_{50} of ormeloxifene was 20 μmol/L in PC3 cells and 15 μmol/L in DU145 cells after 48 hours treatment, respectively (Fig. 1Ai–ii). We next evaluated the effect of ormeloxifene treatment on prostate cancer cell proliferation using xCELLigence assay for the duration of 72 hours (Fig. 1Bi–ii). This assay monitors cell growth in real time by measuring changes in electric impedance between two golden electrodes embedded in the bottom of the cell culture wells. The impedance, which is converted to a cell index value, is directly proportional to the number of cells and also reflects the cells viability, morphology, and adhesion strength (23). The growth curve, which is presented as a baseline cell index, showed that ormeloxifene (10–20 μmol/L) reduced the baseline cell index in PC3 (Fig. 1Bi) and DU145 (Fig. 1Bii) cells in a dose-dependent manner compared with vehicle-treated cells. Ormeloxifene treatment inhibited clonogenic potential of PC3 (Fig. 1Ci–ii), DU145 (Fig. 1Di–ii), and C4-2 (Supplementary Fig. S2Ai–ii) cells as determined by independent colony formation assay. Moreover, ormeloxifene also inhibited anchorage-dependent growth of C4-2 cells (Supplementary Fig. S2Bi–ii). These results indicate that ormeloxifene effectively inhibits growth of prostate cancer cells including highly aggressive metastatic prostate cancer cells.

Ormeloxifene represses β-catenin signaling in prostate cancer cells

As ormeloxifene inhibited proliferation of prostate cancer cells, thus, we examined the effect of ormeloxifene on β-catenin signaling which is a major oncogenic pathway involved in tumorigenesis and metastasis (3, 24–27). Ormeloxifene treatment (10 μmol/L) inhibited nuclear β-catenin in DU145 cells (Fig. 2Ai) through its sequestration in the cytoplasm (Fig. 2Ai) as determined by Western blot analysis. This result was further confirmed by confocal microscopy as ormeloxifene showed inhibition of β-catenin translocation into the nucleus of prostate cancer cells as compared with control (Fig. 2Aii and Supplementary Fig. S3Bi–ii). We next evaluated the effect of ormeloxifene on lithium chloride (LiCl)-induced β-catenin/TCF promoting activity by transiently cotransfecting the DU145 cells with TCF-firefly luciferase reporter constructs (pTOP-FLASH) and *Renilla* luciferase or (pFOP-FLASH) and *Renilla* luciferase. Ormeloxifene treatment (10 μmol/L) for 6 hours, significantly ($P < 0.01$) inhibited lithium chloride (LiCl)-induced TCF-4 promoter activity in DU145 cells (Fig. 2iii). We also examined the effect of ormeloxifene on activation of GSK3β by Western blot analysis which illustrated a marked increase in phosphorylated GSK3β protein levels in DU145 cells (Fig. 2Bi). Because we observed activation of GSK3β protein by ormeloxifene treatment, thus, we next examined the effect of ormeloxifene on β-catenin degradation after using translational inhibitor (cycloheximide). Results revealed a time-dependent decrease in the protein levels of β-catenin in DU145 cells compared with cyclohexamide treatment alone group (Fig. 2Bii–iii). We next performed molecular docking studies to determine the orientation of ormeloxifene bound in the active sites of β-catenin and GSK3β using Discovery Studio software (version 3.5) as described (17). This study revealed that ormeloxifene binds with both β-catenin and GSK3β with a considerably high binding energy. Ormeloxifene binds into the active site of β-catenin (4DJS) and GSK3β (4ACH) with minimum binding energy (ΔG), −6.2 and -8.5 kcal/mol, respectively (Table inserted as Fig. 2C). The docking results also confirmed that ormeloxifene strongly binds with amino acid residue of β-catenin at ARG: 469, ARG: 612 (Fig. 2Di–ii), and GSK3β at LYS: 85, ARG 96 (Fig. 2Diii–iv). These amino acid residues actively participate in hydrophobic, hydrophilic, and π–π interactions. Overall, these results suggest that ormeloxifene is a potent inhibitor of WNT/β-catenin signaling pathway.

Ormeloxifene treatment effectively attenuates metastatic potential of prostate cancer cells

EMT is the basic characteristic of cancer cell in which epithelial cells undergo morphologic and molecular changes that transform these cells to mesenchymal, highly metastatic (invasive and motile) and drug-resistant phenotype (28). Thus, targeting EMT will reduce the invasive phenotypes of a cancer cell and have significant advantage to overcome drug resistance. It has been reported that β-catenin is involved in invasion and metastasis via inducing EMT in various tumor cells including prostate cancer (29, 30). Because ormeloxifene effectively inhibits β-catenin signaling, therefore, we evaluated the effect of ormeloxifene treatment on various EMT markers in prostate cancer cells. Ormeloxifene treatment revealed marked inhibition of N-cadherin, and Snail expressions in PC3 and DU145 cells (Fig. 3Ai–ii), whereas it induced the expression of E-cadherin in PC3 prostate cancer cells (Fig. 3Ai). Activation of MMPs are involved in matrix degradation that facilitate invasion of cancer cells (31), thus we sought to investigate the effect of ormeloxifene treatment on MMPs and found that ormeloxifene inhibited the expression of MMP2 and MMP3 (Fig. 3Ai–ii). We next performed functional assays (invasion and migration) by Boyden's chamber to determine whether ormeloxifene inhibits the invasive and migratory potential of prostate cancer cells. Our results revealed that ormeloxifene treatment (5–15 μmol/L) effectively inhibited both invasion (Fig. 3Bi) and migration (Fig. 3Ci) of PC3 cells and C4-2 cells (Supplementary Fig. S2Ci–ii). We further investigated the impact of ormeloxifene on real-time invasion and migration of PC3 cells using xCELLigence system. Ormeloxifene treatment also effectively decreased invasion (Fig. 3Bii) and migration (Fig. 3Cii) of PC3 cells. We further confirmed effect of ormeloxifene on PC3 cells migration (Fig. 3D) by beads assay. Our results revealed a marked decrease in number of migratory PC3 cells after 48 hours ormeloxifene treatment compared with control group (Fig. 3D).

Ormeloxifene treatment arrests cell cycle via modulation of cell-cycle regulatory proteins

Various studies have shown that agents which arrest cell cycle in G_0–G_1 phase have potential chemotherapeutic effects (32, 33). Because, we observed that ormeloxifene inhibits the growth of prostate cancer cells, we sought to determine the effect of ormeloxifene on prostate cancer cell-cycle distribution. For this, we synchronized PC3 cells and treated with ormeloxifene (10–20 μmol/L) for 24 hours and cell-cycle analysis was performed by flow cytometry. Ormeloxifene treatment arrested PC3 cells cycle in G_0–G_1 phase in a dose-dependent manner (Fig. 4Ai–ii). Ormeloxifene treatment resulted in 5%, 20%, and 20% increase in cell-cycle arrest in G_0–G_1 phase at 10, 15, and 20 μmol/L dose, respectively, compared with vehicle-control treated cells (insert Table in Fig. 4Aii). Similar result was also observed in DU145 cells (Supplementary Fig. S3). We then evaluated the effect of ormeloxifene on cell-cycle regulatory proteins in prostate cancer cells. Ormeloxifene (10–20 μmol/L) inhibited expression of Mcl-1 in both PC3 and DU145 cells (Fig. 4Bi–ii). However, ormeloxifene (10–20 μmol/L) treatment showed more effect on cyclin D1 inhibition in DU145-treated cells as compared with PC3-treated

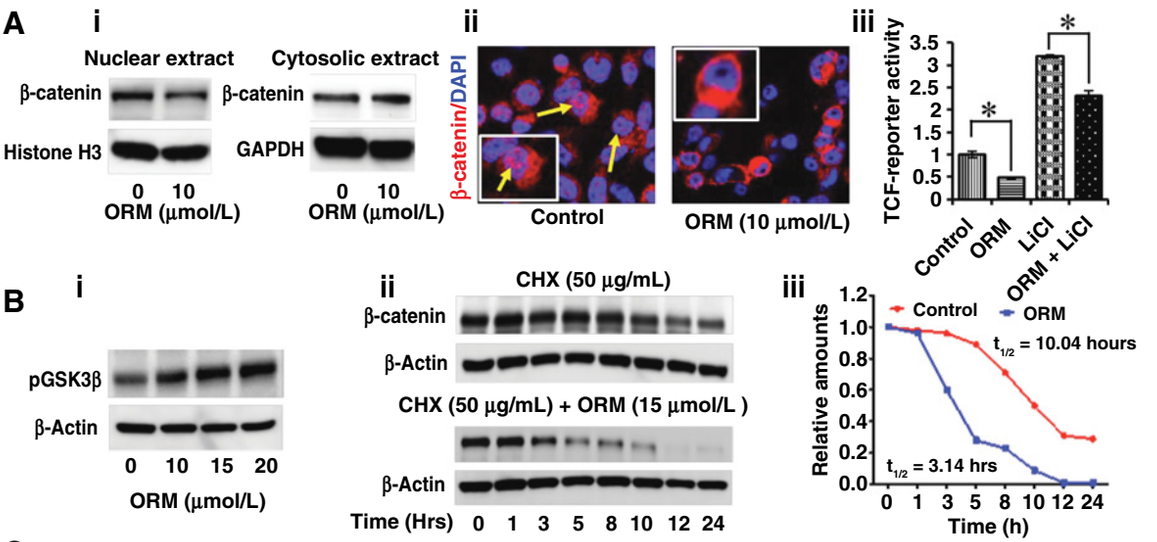

C

Compound	Protein	Binding energy (kcal/mol)	No. of hydrogen bonds	Hydrogen bond forming residues	Distance (Å)	π-π Interactions
ORM	β-catenin (4DJS)	–6.2	3	ARG 469, ARG 612	3.0, 3.1 3.5	ARG 469, ARG 612
	GSK3β (4ACH)	–8.5	1	ARG 96	3.2	ARG96, LYS85

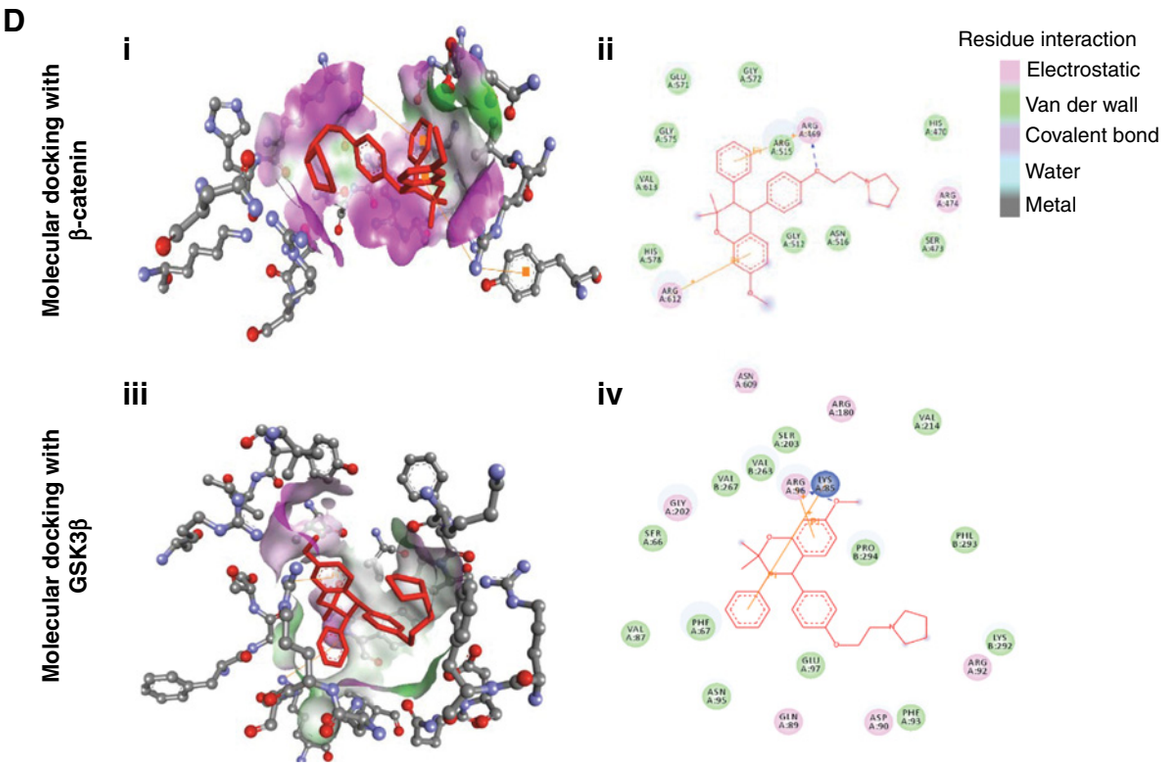

cells. Ormeloxifene treatment induced expression of cell-cycle inhibitory proteins (p21 and p27) in both PC3 and DU145 cells (Fig. 4Bi–ii). These results suggest that ormeloxifene arrests cell cycle via modulating key cell-cycle regulatory proteins.

Ormeloxifene treatment induces apoptosis in prostate cancer cells

Because we observed arrest of cell cycle in G_0–G_1 phase, thus we investigated the effect of ormeloxifene on apoptotic induction in prostate cancer cells by flow cytometry analysis. Ormeloxifene (10–20 μmol/L) dose-dependently increased apoptotic cell populations in both PC3 (Fig. 5Ai) and DU145 (Fig. 5Aii) cells as determined by enhanced Annexin V positive cells. Ormeloxifene at 20 μmol/L showed 55.6% and 50% apoptotic PC3 and DU145 cells respectively compared with control group (Fig. 5Ai–ii). We next examined the effect of ormeloxifene on mitochondrial membrane potential ($\Delta\psi m$) using TMRE staining (Fig. 5Bi–ii), which is a marker of apoptosis induction through intrinsic pathway. Ormeloxifene (10–20 μmol/L) dose-dependently decreased TMRE staining in both DU145 and PC3 cells as determined by fluorescence microscopy (Fig. 5Bi) and flow cytometry (Fig. 5Bi–ii), respectively. We also examined the effect of ormeloxifene on PARP cleavage which is a marker for apoptosis. Ormeloxifene (20 μmol/L) induced PARP cleavage as determined by Western blot analysis (Fig. 5C). These results suggest apoptosis inducing potential of ormeloxifene in prostate cancer cells.

Ormeloxifene suppresses tumor growth in xenograft mouse model

To evaluate clinical relevance of our *in vitro* findings, we subcutaneously implanted PC3 cells in a preclinical xenograft mouse model. Intraperitoneal administration of ormeloxifene (250 μg/mice/thrice weekly) significantly ($P < 0.01$) reduced prostate cancer tumor growth (Fig. 6Ai–iii). To confirm if this tumor growth inhibition is mediated through the suppression of β-catenin, we performed immunofluorescence analysis of excised xenograft tumors for β-catenin. Both cytoplasmic and nuclear β-catenin expression was decreased in ormeloxifene-treated xenograft tumor cells compared with control tumor cells (Fig. 6B). This result was validated by immunohistochemistry analysis (Fig. 6C). We further determined the expression of EMT markers in excised tumor tissues of control and ormeloxifene-treated mice. Ormeloxifene treatment also inhibited the expression of N-cadherin, Slug, Snail, and Vimentin and induced the expression of E-Cadherin (Fig. 6C). Metastasis-associated protein 1 (MTA1) is known to be upregulated in many cancer types and is an important metastatic marker for tumor aggressiveness and metastasis (34, 35). Interestingly, we observed a decreased expression of MTA1 in ormeloxifene-treated xenograft tissues as compared with control. Next, we examined the expression of cell proliferative markers, proliferative cell nuclear antigen (PCNA), in control and ormeloxifene-treated tumor tissues by immunohistochemistry analysis. We found a marked decrease in nuclear PCNA staining in ormeloxifene-treated tumors compared with the tumors in vehicle-treated mice (Fig. 6C). These results reaffirm that ormeloxifene has potent therapeutic efficacy against prostate cancer and could be used for the treatment of metastatic prostate cancer. The possible molecular mechanisms of ormeloxifene to inhibit prostate tumor growth and metastasis have been summarized in a schematic diagram (Supplementary Fig. S4), which shows ormeloxifene inhibits Wnt/β-catenin and EMT signaling and it induces activation of GSK3β, E-cadherin, p21, and p27 signaling pathways, thus decreasing prostate tumor growth and metastasis.

Discussion

Prostate cancer continues to remain the most common cancer and the second leading cause of cancer-related deaths, in American men. Metastatic prostate cancer is the end-stage and accounts for the majority of cancer deaths (22). Moreover, men with metastatic prostate cancer are at a higher risk of developing bone metastasis, which results in clinical skeletal morbidity (36). Although prostate cancer is frequently curable in its early stage by surgical and/or radiation therapy, many patients present locally advanced or metastatic disease for which there are currently no curative treatment options (37). Docetaxel and Cabazitaxel are FDA approved chemotherapeutic drugs for the treatment of metastatic prostate cancer, but these drugs have severe toxic side effects (38, 39). Accumulating evidence suggest that β-catenin signaling pathway and its related oncogenic events play a major role during the development, progression, and metastasis of cancer including prostate cancer (30, 40). Thus, there is an urgent need to identify more effective and nontoxic agents or drugs, which can target Wnt/β-catenin and related oncogenic pathways.

Figure 2.

Effect of ormeloxifene on β-catenin signaling pathway and molecular docking of ormeloxifene (ORM) with β-catenin and GSK3β. **A,** Effect of ormeloxifene on β-catenin distribution in cytoplasm and nucleus of DU145 cells. Briefly, cells were treated with indicated concentrations of ormeloxifene for 24 hours, nuclear extracts were prepared and subjected for Western blot analysis to detect the protein levels of β-catenin. Results demonstrating decreased expression of nuclear β-catenin and increased expression of β-catenin in the cytoplasm (**Ai**) of DU145 cells. Blots were reprobed with Histone H3 and GAPDH antibodies as an internal control. Effect of ormeloxifene on β-catenin localization in PC3 cells as determined by confocal microscopy (**Aii**). Yellow arrows indicate localization of β-catenin in control and ormeloxifene-treated cells after 24 hours treatment (original magnification 40×) (**Aii**). Effect of ormeloxifene on TCF-4 promoter activity (**Aiii**). Cells were transiently cotransfected with TCF-firefly luciferase reporter constructs (pTOP-FLASH; 1 μg) and *Renilla* luciferase (200 ng) or (pFOP-FLASH; 1 μg) and *Renilla* luciferase (200 ng). After 24 hours, cells were treated with LiCl (50 μmol/L) alone or in combination with ormeloxifene (10 μmol/L). Cell lysates were prepared 6 hours posttreatment and firefly and *Renilla* luciferase activity was analyzed by using Dual Luciferase Kit (Promega). The β-catenin/TCF transcription activity was determined by normalizing the firefly luciferase activity to that of *Renilla* luciferase activity and calculating the ratio of TOP-FLASH signal to FOP-FLASH signal. Values in bar graph indicates mean ± SE of three wells reading in each group. Asterisk (*) denotes the significant value $P < 0.01$. **B,** Effects of ormeloxifene on protein levels of phospho GSK3β in DU145 as determined by Western blot analysis (**Bi**). Effect of ormeloxifene on β-catenin degradation as analyzed by pulse chase experiment. Briefly, DU145 cells were treated with cycloheximide (CHX; 50 μg) alone or in combination with ormeloxifene (15 μmol/L) at indicated time points. Protein lysates were prepared and subjected for Western blot analysis to analyze the protein levels of β-catenin. Results indicates protein levels of β-catenin in alone cyclohexamide-treated (top blot) and in cycloheximide and ormeloxifene-treated (bottom blot) (**Bii**). Line graph showing quantification of Western blots of **Bii**. $T_{1/2}$ denotes time point for 50% β-catenin degradation. **C** and **D,** Molecular docking studies of ormeloxifene with β-catenin and GSK3β. **C,** Table showing docking score of ormeloxifene with β-catenin and GSK3β. **D,** Stereo view of ormeloxifene binding with β-catenin (**Di**) and GSK3β (**Diii**) showing hydrogen bond donor and acceptor residues around component. Schematic diagram of ormeloxifene docking with β-catenin (**Dii**) and GSK3β (**Div**) showing residues involved in hydrogen-bonding, Pi interactions, charge or polar interactions, Van der Waals interactions, which are represented by respective colors.

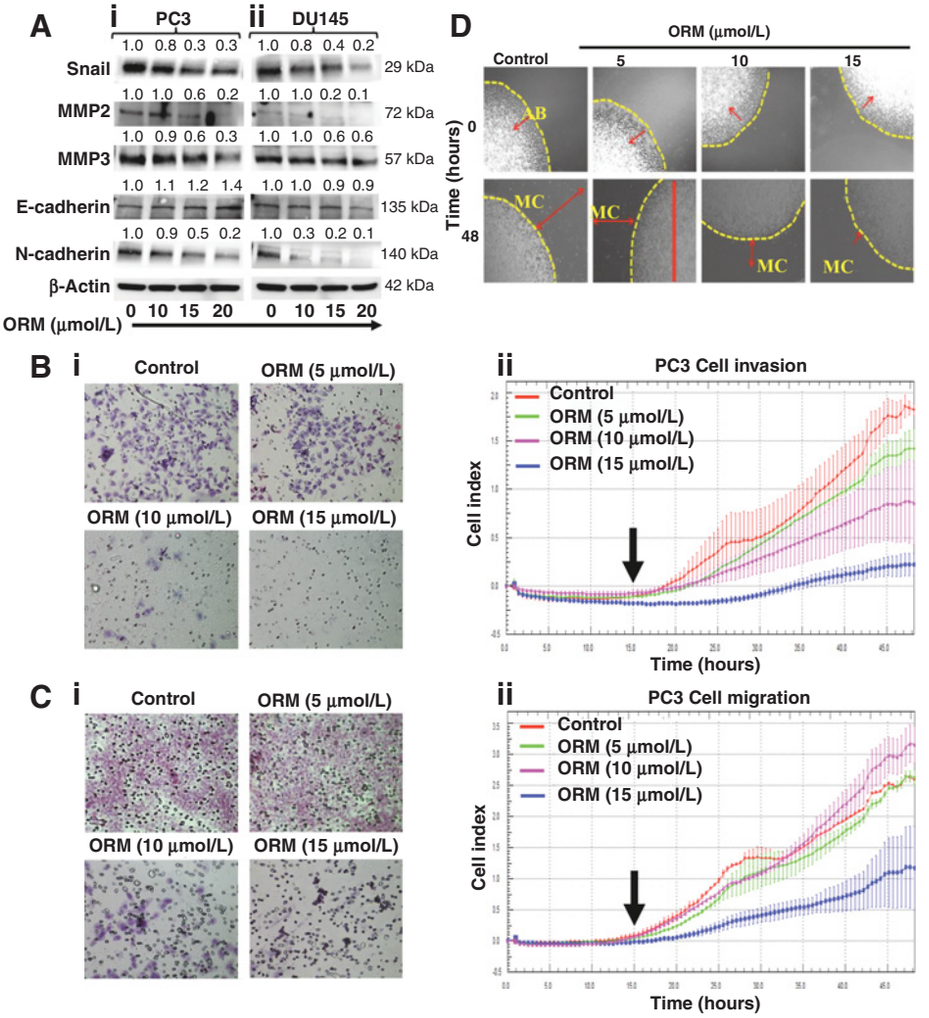

Figure 3.

Effect of ormeloxifene (ORM) on cell invasion, migration, and EMT markers. Briefly, 70% confluent prostate cancer cells were treated with ormeloxifene (10–20 μmol/L) for 24 hours. Cell lysates were prepared and subjected for Western blot analysis for EMT markers and MMPs analysis. **A,** Effect of ormeloxifene on EMT markers (E-cadherin, N-cadherin, and Snail) and MMPs (MMP2 and MMP3) in PC3 (**i**) and DU145 (**ii**) cells. Values shown above the blots are the densitometry analysis of each protein band normalized with respective β-actin value. **B,** Effect of ormeloxifene on invasion of PC3 cells as determined by Boyden chamber and xCELLigence assays. Representative photographs (20× original magnification) of invaded cells of control and ormeloxifene-treated PC3 cells as determined by Boyden Chamber Kit (**i**). Effect of ormeloxifene on real-time cell invasion (**ii**). Briefly, PC3 cells (7×10^4) were seeded in invasion plate and invasion potential of these cells was determined by xCELLigence instrument as described in material and methods. Results indicate dose-dependent decrease in Cell Index, which correlates inhibition of real-time cell invasion by ormeloxifene treatment (**ii**). C, Effect of ormeloxifene on cell migration of PC3 cells as determined by Boyden chamber and xCELLigence assays. Representative images (20× original magnification) showing inhibition of PC3 cells migration by Boyden chamber assay (**i**). Effect of ormeloxifene on real-time cell migration as determined by xCELLigence assay (**ii**). Briefly, PC3 cells (7×10^4) were seeded in migration plate and ormeloxifene treatment (5–15 μmol/L) was given after 15 hours and allowed the plate at 37 °C and 5% CO_2 for real-time migration assay up to 48 hours. Results indicate significant decrease in migratory potential of ormeloxifene treated PC3 cells compared with control. **D,** Effect of ormeloxifene on motility potential of PC3 cells as determined by agarose bead assay. Representative images of migratory cells (MC) in control and ormeloxifene-treated groups at 0 and 48 hours. AB denotes agarose beads. Images were captured at 4× magnification.

Ormeloxifene has an excellent therapeutic index and is safe for chronic administration in humans (14). The maximum serum concentration (C_{max}) of ormeloxifene in humans is dose dependent (C_{max} of 55.53 ± 15.43 ng/mL for 30 mg dose and C_{max} of 122.57 ± 6.25 ng/mL for 60 mg dose) and is reached within 4 to 6 hours (41). Similar C_{max} values for ormeloxifene has also been detected in breast cancer patients treated with either 30 mg, twice a week for 12 weeks (C_{max} 54.98 ± 14.19 ng/mL) or 60 mg of ormeloxifene on alternate days for 1 month (C_{max} 135 ± 15.5 ng/mL). These studies indicate that ormeloxifene is a nontoxic, highly bioavailable, and shown potent anticancer effects against breast cancer (10), HNSCC (11), ovarian (12), and pancreatic cancer (13). However, molecular mechanisms of its anticancer properties are not well understood. In this study, we identified a novel molecular mechanism of ormeloxifene's anticancer action as it effectively targets Wnt/β-catenin and EMT-related oncogenic signaling pathways in prostate cancer cells.

A i

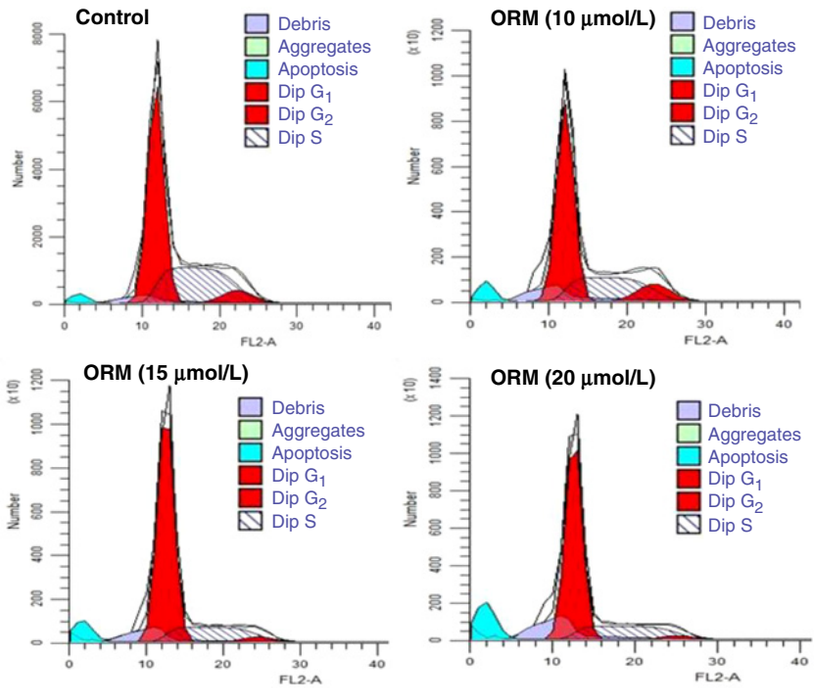

ii

Groups	G_0–G_1	S	G_2–M
Control	55.0 ± 1.12	38.4 ± 1.27	6.6 ± 0.31
ORM (10 mol/L)	59.8 ± 4.69	24.4 ± 6.48	15.8 ± 3.10
ORM (15 mol/L)	75.5 ± 0.05	21.2 ± 0.14	3.2 ± 0.11
ORM (20 mol/L)	74.6 ± 0.52	21.9 ± 0.66	3.4 ± 0.57

B

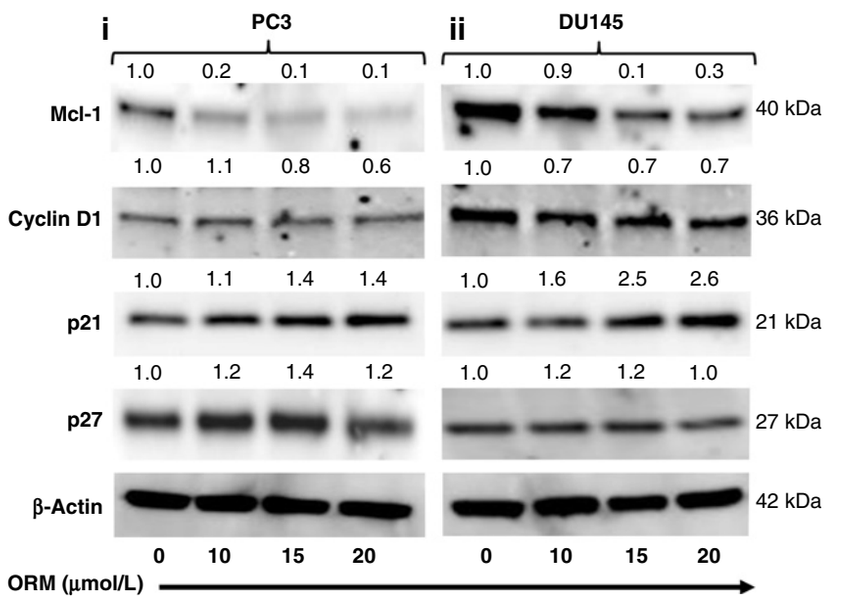

Figure 4.
Effect of ormeloxifene (ORM) on cell-cycle progression of prostate cancer cells. Ormeloxifene arrests PC3 cell cycle in G_0–G_1 phase as determined by flow cytometry. **A,** Histogram (i) and table (ii) represent the cell-cycle distribution in PC3 cells. **B,** Effect of ormeloxifene on protein levels of cell-cycle regulatory proteins (cyclin D1, Mcl-1, p21, and p27) in both PC3 (**Bi**) and DU145 (**Bii**) cells. Briefly, cells were treated with indicated concentrations of ormeloxifene for 24 hours, total cell lysates were prepared, and subjected for Western blot analysis. Equal loading of protein in each lane was determined by probing the blots with β-Actin antibody. Values shown above the blots are the densitometry analysis of each protein band normalized with respective β-Actin value.

It is well documented that constitutive activation of β-catenin signaling pathway plays a major role in cancer progression and metastasis (3, 24) and drug resistance (42). Accumulating evidences also suggest that β-catenin cross-talks with other oncogenic signaling components leading to more aggressive phenotype of prostate cancer cells (43). GSK3β-dependent phosphorylation of

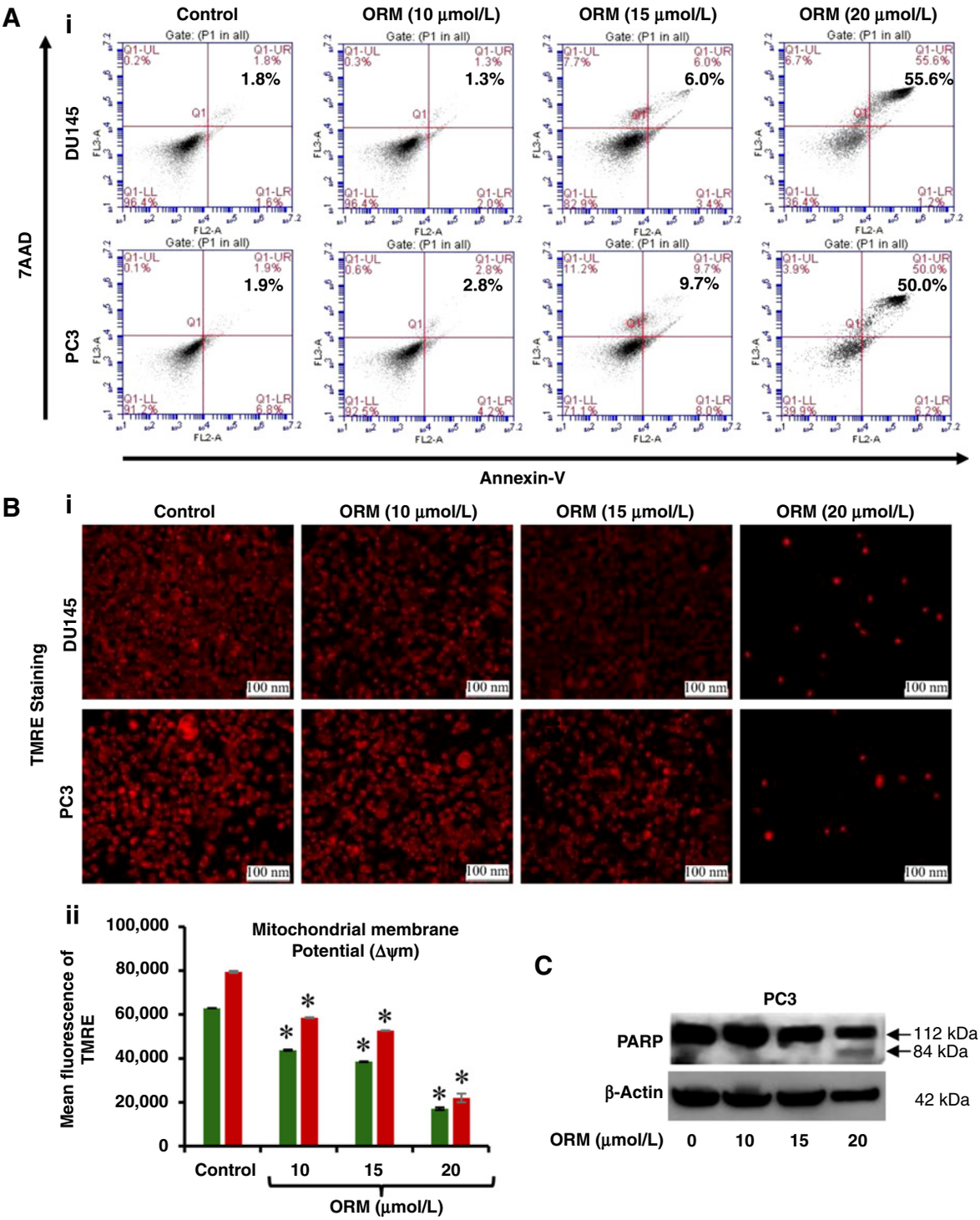

Figure 5.

Ormeloxifene (ORM) treatment induces apoptosis in prostate cancer cells. PC3 and DU145 cells were treated with indicated concentration of ormeloxifene for 24 hours and processed for apoptosis analysis using Annexin V-7AAD Apoptosis Kit. **A,** Representative FL3-A and FL2-A plots showing dose-dependent increase of apoptosis in DU145 (**i**) and PC3 cells (**ii**). **B,** Effect of ormeloxifene on mitochondrial membrane potential (Δψm) as determined by TMRE staining. Representative fluorescence images showing dose-dependent effect of ormeloxifene on TMRE staining in PC3 and DU145 cells (**i**). Bar graph indicating dose-dependent inhibition of mitochondrial membrane potential (Δψm) in ormeloxifene-treated PC3 and DU145 cells as determined by flow cytometry. Asterisk (*) denotes the significant value $P < 0.01$. **C,** Effect of ormeloxifene on PARP cleavage. Briefly, 70% confluent prostate cancer cells were treated with ormeloxifene (10–20 μmol/L) for 24 hours. Whole cell lysates was prepared and subjected for Western blot analysis for full and cleaved PARP.

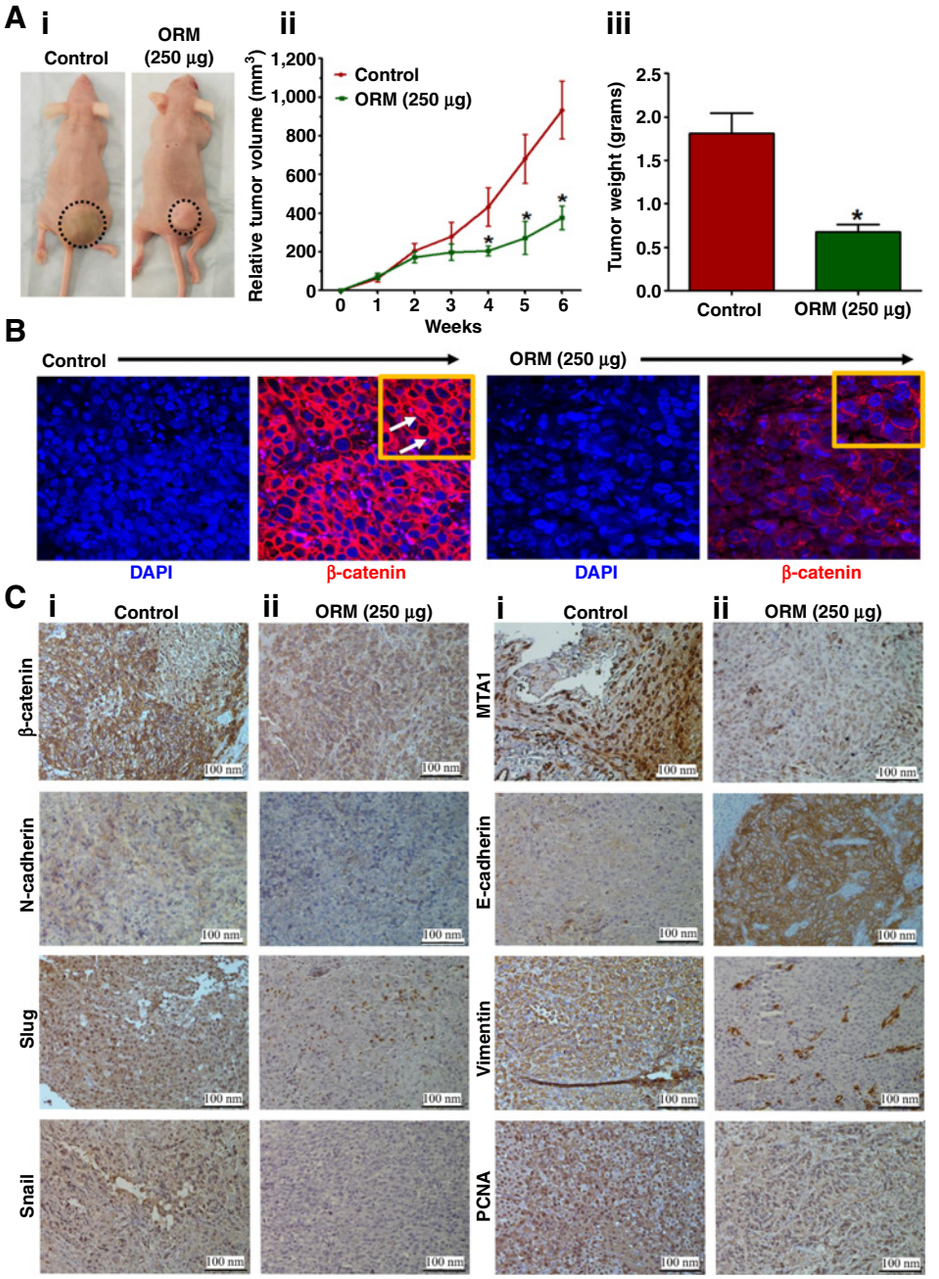

Figure 6.

Ormeloxifene (ORM) inhibits prostate tumor growth in xenograft mouse model. **A,** Effect of ormeloxifene on PC3 cells derived xenograft tumors in athymic nude mice. In brief, a total of 12 mice were used in this experiment and were divided into two groups. A total of 2×10^6 PC3 cells were injected subcutaneously on dorsal flank of each mouse. Ormeloxifene (250 μg) was administered (intraperitoneal; 250 μg/mouse) thrice a week till 6 weeks and control group mice received 0.2% ethanol in PBS as vehicle control. Mice of both the groups were sacrificed when control mice reached a targeted tumor volume of 1,000 mm^3. Representative mouse picture of control and ormeloxifene-treated tumor bearing mouse (**i).** Average tumor volume of each group mice at different weeks (**ii).** Bar graph representing tumor weight of each group mice (**iii**). Value in graph represents mean ± SE of six mice in each group. Asterisk (*) denotes the significant value $P < 0.01$. **B,** Effect of ormeloxifene on β-catenin expression in xenograft tumors of control and ormeloxifene-treated mice as determined by immunofluorescence (IF) analysis. White arrows indicate β-catenin accumulation in nucleus of the xenograft tissues. **C,** Effect of ormeloxifene on the expressions of β-catenin, N-cadherin, MTA1, Slug, Snail, Vimentin, and E-cadherin and PCNA in excised tumors of control (**i**) and ormeloxifene (**ii**) treated mice as determined by IHC analysis. All images of IF and IHC analyses were captured at 20× magnification.

β-catenin enhances its proteasomal degradation and inhibits its translocation into the nucleus, thus regulates its various downstream target oncogenes. Our results indicate that ormeloxifene activates GSK3β, thereby, degrades β-catenin in the cytoplasm and also inhibits nuclear β-catenin translocation and represses TCF-4 promoter activity. It has been reported that ARG 469 is one of the important amino acids involved in β-catenin interaction with TCF4 (44). Our molecular docking results indicate that ormeloxifene potentially binds with ARG 469 amino acids of β-catenin (Fig. 2Di). It is possible that ormeloxifene inhibits β-catenin induced TCF4 promoter activity *via* binding to this cavity and inhibiting β-catenin/TCF4 interaction. Both LYS 85 and ARG 96 are important amino acids for GSK3β, which plays an important role in ATP binding and phosphoryl transfer (45, 46). It has been documented that mutation of LYS85 with ARG inhibits binding of Axin to GSK3β, which resulted in inactivation of GSK3β (47). Mutation in ARG 96 leads to complete loss of GSK3β catalytic activity (46). Consistent with this observation, our molecular docking study reveals that ormeloxifene effectively docks with LYS 85 and ARG 96 (Fig. 2Dii). It may be possible that ormeloxifene induces activation of GSK3β through increased ATP binding at LYS 85 and blocking mutation in these amino acids. More biological studies are warranted to further confirm the importance of these amino acid residues in ormeloxifene-induced activation of GSK3β. β-catenin also regulates EMT-related oncogenic signaling though which cancer cells gain mesenchymal and metastatic

characteristics (48). EMT is typically accompanied by loss of epithelial markers such as E-cadherin and gain of mesenchymal markers such as N-cadherin, Snail, and Vimentin in prostate cancer (49, 50). Our results indicate that ormeloxifene induces the expression of E-cadherin and inhibits Snail and N-cadherin in prostate cancer cells. These results suggest that ormeloxifene effectively blocks EMT progression. MMPs are secreted proteins which help cancer cell to invade through basal lamina by degrading extracellular matrix (51). MMP2/3 plays an important role in progression and metastasis of prostate cancer (31). Our results indicate that ormeloxifene has the ability to inhibit metastatic potential of prostate cancer cells, through repression of MMP2 and MMP3. In this study, we have also shown that ormeloxifene can effectively inhibit the cell proliferation and clonogenic potential of highly aggressive prostate cancer cells. Abnormal regulation of cell-cycle progression is one of trademark of cancer cells (52). G_0–G_1 abrogation of the cell cycle prevents cancer cells from repairing DNA and inhibits them from entering the S phase. Thus, the G_0–G_1 checkpoint has emerged as an attractive therapeutic target for cancer therapy (32). Interestingly, ormeloxifene treatment arrested prostate cancer cells in in G_0–G_1 phase of cell cycle and induced apoptosis. These results are consistent with similar previous findings in other cancer cells (12, 13). It has been shown that cyclins and cyclin-dependent kinases (CDK) play a critical role in cell-cycle progression; their deregulation leads to cell-cycle arrest (53). The observed inhibitory effects of ormeloxifene on cyclin D1 in prostate cancer cells clearly demonstrates interference in cell-cycle regulatory proteins. It is known that p21/WAF1 and p27/KIP1 regulates CDK activity and our results illustrate increased expression of both p21 and p27 proteins in prostate cancer cells. These results suggest that ormeloxifene has the ability to arrest the prostate cancer cells in G_0–G_1 phase via modulating cell-cycle regulatory proteins. Thus, ormeloxifene is expected to have high therapeutic efficacy against prostate cancer. Our *in vivo* therapeutic study showed that ormeloxifene significantly ($P < 0.01$) reduces the prostate tumors burden in the preclinical athymic nude mouse model with no apparent toxicity. We also observed effective inhibition of β-catenin and EMT related markers (vimentin, N-cadherin, snail, and slug) in excised xenograft tumors of ormeloxifene-treated mice. It has been reported that MTA1 and β-catenin reciprocally activate each other during cancer/metastasis progression (54, 55). Inhibition of MTA1 expression correlates with improved clinical outcome in various cancer types. Ormeloxifene-mediated repression of MTA1 in xenograft tumors further indicates its potential to inhibit prostate cancer metastasis. Taken together, these results confirm that ormeloxifene is a potent inhibitor of β-catenin and EMT-related signaling pathways and has a potential to inhibit the metastatic phenotype of prostate cancer cells. These results also suggest that ormeloxifene can be repurposed for the treatment of metastatic prostate cancer. For that, human trials, however, are warranted in near future.

Conclusion

In summary, we have shown potential anticancer effects of ormeloxifene against prostate cancer using cell lines and preclinical mouse models. ormeloxifene efficiently targets β-catenin and EMT-related signaling pathways to repress prostate tumor growth and metastatic phenotypes. We conclude that ormeloxifene could be used alone or in combination with current therapeutic regimen for the treatment of human prostate cancer.

Disclosure of Potential Conflicts of Interest

No potential conflicts of interest were disclosed.

Authors' Contributions

Conception and design: B.B. Hafeez, F.T. Halaweish, N. Zafar, S.C. Chauhan, M. Jaggi

Development of methodology: B.B. Hafeez, N. Chauhan, S. Malik, A.E. Massey, F.T. Halaweish, N. Zafar, M.M. Yallapu, S.C. Chauhan

Acquisition of data (provided animals, acquired and managed patients, provided facilities, etc.): B.B. Hafeez, A. Ganju, M. Sikander, V.K. Kashyap, N. Chauhan, A.E. Massey, F.T. Halaweish, N. Zafar, S.C. Chauhan, M. Jaggi

Analysis and interpretation of data (e.g., statistical analysis, biostatistics, computational analysis): B.B. Hafeez, A. Ganju, N. Chauhan, A.E. Massey, M.K. Tripathi, F.T. Halaweish, S.C. Chauhan

Writing, review, and/or revision of the manuscript: B.B. Hafeez, A. Ganju, N. Chauhan, F.T. Halaweish, N. Zafar, M.M. Singh, M.M. Yallapu, S.C. Chauhan, M. Jaggi

Administrative, technical, or material support (i.e., reporting or organizing data, constructing databases): N. Chauhan, A.E. Massey, N. Zafar, M.M. Yallapu, S.C. Chauhan

Study supervision: B.B. Hafeez, S.C. Chauhan, M. Jaggi

Other (performed and analyzed the docking study): Z.B. Hafeez

Acknowledgments

The authors would like to thank Dr. R. Moon (University of Washington, Seattle, WA) for providing TCF/LIF constructs. Confocal microscopy studies were conducted at the imaging core in the Neuroscience Department at The University of Tennessee Health Science Center.

Grant Support

This work was supported by Department of Defense (DOD) grant W81XWH-14-1-0154; NIH U01CA162106, NIH R01CA142736, and College of Pharmacy/University of Tennessee Health Science Center Seed grant.

The costs of publication of this article were defrayed in part by the payment of page charges. This article must therefore be hereby marked *advertisement* in accordance with 18 U.S.C. Section 1734 solely to indicate this fact.

Received February 17, 2017; revised April 21, 2017; accepted May 22, 2017; published OnlineFirst June 14, 2017.

References

1. Siegel RL, Miller KD, Jemal A. Cancer Statistics, 2017. CA Cancer J Clin 2017;67:7–30.
2. Silvestris N, Leone B, Numico G, Lorusso V, De Lena M. Present status and perspectives in the treatment of hormone-refractory prostate cancer. Oncology 2005;69:273–82.
3. Chen G, Shukeir N, Potti A, Sircar K, Aprikian A, Goltzman D, et al. Up-regulation of Wnt-1 and beta-catenin production in patients with advanced metastatic prostate carcinoma: potential pathogenetic and prognostic implications. Cancer 2004;101:1345–56.
4. Jaggi M, Nazemi T, Abrahams NA, Baker JJ, Galich A, Smith LM, et al. N-cadherin switching occurs in high Gleason grade prostate cancer. Prostate 2006;66:193–9.
5. Jaggi M, Johansson SL, Baker JJ, Smith LM, Galich A, Balaji KC. Aberrant expression of E-cadherin and beta-catenin in human prostate cancer. Urol Oncol 2005;23:402–6.
6. De P, Carlson JH, Wu H, Marcus A, Leyland-Jones B, Dey N. Wnt-beta-catenin pathway signals metastasis-associated tumor cell phenotypes in triple negative breast cancers. Oncotarget 2016;7:43124–49.

7. Novak A, Dedhar S. Signaling through beta-catenin and Lef/Tcf. Cell Mol Life Sci 1999;56:523–37.
8. Chesire DR, Ewing CM, Gage WR, Isaacs WB. In vitro evidence for complex modes of nuclear beta-catenin signaling during prostate growth and tumorigenesis. Oncogene 2002;21:2679–94.
9. Heuberger J, Birchmeier W. Interplay of cadherin-mediated cell adhesion and canonical Wnt signaling. Cold Spring Harbor Perspect Biol 2010;2: a002915.
10. Nigam M, Ranjan V, Srivastava S, Sharma R, Balapure AK. Centchroman induces G0/G1 arrest and caspase-dependent apoptosis involving mitochondrial membrane depolarization in MCF-7 and MDA MB-231 human breast cancer cells. Life Sci 2008;82:577–90.
11. Srivastava VK, Gara RK, Bhatt ML, Sahu DP, Mishra DP. Centchroman inhibits proliferation of head and neck cancer cells through the modulation of PI3K/mTOR pathway. Biochem Biophys Res Commun 2011;404:40–5.
12. Maher DM, Khan S, Nordquist JL, Ebeling MC, Bauer NA, Kopel L, et al. Ormeloxifene efficiently inhibits ovarian cancer growth. Cancer Lett 2015;356:606–12.
13. Khan S, Ebeling MC, Chauhan N, Thompson PA, Gara RK, Ganju A, et al. Ormeloxifene suppresses desmoplasia and enhances sensitivity of gemcitabine in pancreatic cancer. Cancer Res 2015;75:2292–304.
14. Singh MM. Centchroman, a selective estrogen receptor modulator, as a contraceptive and for the management of hormone-related clinical disorders. Med Res Rev 2001;21:302–47.
15. Sikander M, Hafeez BB, Malik S, Alsayari A, Halaweish FT, Yallapu MM, et al. Cucurbitacin D exhibits potent anti-cancer activity in cervical cancer. Sci Rep 2016;6:36594.
16. Khan S, Sikander M, Ebeling MC, Ganju A, Kumari S, Yallapu MM, et al. MUC13 interaction with receptor tyrosine kinase HER2 drives pancreatic ductal adenocarcinoma progression. Oncogene 2017;36: 491–500.
17. Grossmann TN, Yeh JT-H, Bowman BR, Chu Q, Moellering RE, Verdine GL. Inhibition of oncogenic Wnt signaling through direct targeting of β-catenin. Proc Natl Acad Sci 2012;109:17942–7.
18. Berg S, Bergh M, Hellberg S, Högdin K, Lo-Alfredsson Y, Söderman P, et al. Discovery of novel potent and highly selective glycogen synthase kinase-3β (GSK3β) inhibitors for Alzheimer's disease: design, synthesis, and characterization of pyrazines. J Med Chem 2012;55:9107–19.
19. Fuhrmann J, Rurainski A, Lenhof HP, Neumann D. A new Lamarckian genetic algorithm for flexible ligandreceptor docking. J Comput Chem 2010;31:1911–8.
20. Ansari MF, Siddiqui SM, Ahmad K, Avecilla F, Dharavath S, Gourinath S, et al. Synthesis, antiamoebic and molecular docking studies of furan-thiazolidinone hybrids. Eur J Med Chem 2016;124:393–406.
21. Chauhan SC, Vannatta K, Ebeling MC, Vinayek N, Watanabe A, Pandey KK, et al. Expression and functions of transmembrane mucin MUC13 in ovarian cancer. Cancer Res 2009;69:765–74.
22. Siegel RL, Miller KD, Jemal A. Cancer statistics, 2016. CA Cancer J Clin 2016;66:7–30.
23. Abassi YA, Xi B, Zhang W, Ye P, Kirstein SL, Gaylord MR, et al. Kinetic cell-based morphological screening: prediction of mechanism of compound action and off-target effects. Chem Biol 2009;16:712–23.
24. Morita N, Uemura H, Tsumatani K, Cho M, Hirao Y, Okajima E, et al. E-cadherin and alpha-, beta- and gamma-catenin expression in prostate cancers: correlation with tumour invasion. Br J Cancer 1999;79: 1879–83.
25. Shen T, Zhang K, Siegal GP, Wei S. Prognostic value of E-cadherin and beta-catenin in triple-negative breast cancer. Am J Clin Pathol 2016;46:603–10.
26. Chen Z, He X, Jia M, Liu Y, Qu D, Wu D, et al. beta-catenin overexpression in the nucleus predicts progress disease and unfavourable survival in colorectal cancer: a meta-analysis. PLoS One 2013;8:e63854.
27. Tseng RC, Huang WR, Lin SF, Wu PC, Hsu HS, Wang YC. HBP1 promoter methylation augments the oncogenic beta-catenin to correlate with prognosis in NSCLC. J Cell Mol Med 2014;18:1752–61.
28. Nakazawa M, Kyprianou N. Epithelial-mesenchymal-transition regulators in prostate cancer: androgens and beyond. J Steroid Biochem Mol Biol 2017;166:84–90.
29. Zhao JH, Luo Y, Jiang YG, He DL, Wu CT. Knockdown of beta-Catenin through shRNA cause a reversal of EMT and metastatic phenotypes induced by HIF-1alpha. Cancer Invest 2011;29:377–82.
30. Jiang YG, Luo Y, He DL, Li X, Zhang LL, Peng T, et al. Role of Wnt/beta-catenin signaling pathway in epithelial-mesenchymal transition of human prostate cancer induced by hypoxia-inducible factor-1alpha. Int J Urol 2007;14:1034–9.
31. Stearns M, Stearns ME. Evidence for increased activated metalloproteinase 2 (MMP-2a) expression associated with human prostate cancer progression. Oncol Res 1996;8:69–75.
32. Gupta S, Hussain T, Mukhtar H. Molecular pathway for (-)-epigallocatechin-3-gallate-induced cell cycle arrest and apoptosis of human prostate carcinoma cells. Arch Biochem Biophys 2003;410:177–85.
33. Johnson JJ, Petiwala SM, Syed DN, Rasmussen JT, Adhami VM, Siddiqui IA, et al. alpha-Mangostin, a xanthone from mangosteen fruit, promotes cell cycle arrest in prostate cancer and decreases xenograft tumor growth. Carcinogenesis 2012;33:413–9.
34. Li DQ, Pakala SB, Reddy SD, Peng S, Balasenthil S, Deng CX, et al. Metastasis-associated protein 1 is an integral component of the circadian molecular machinery. Nat Commun 2013;4:2545.
35. Li DQ, Pakala SB, Nair SS, Eswaran J, Kumar R. Metastasis-associated protein 1/nucleosome remodeling and histone deacetylase complex in cancer. Cancer Res 2012;72:387–94.
36. Valdespino V, Tsagozis P, Pisa P. Current perspectives in the treatment of advanced prostate cancer. Med Oncol 2007;24:273–86.
37. So A, Gleave M, Hurtado-Col A, Nelson C. Mechanisms of the development of androgen independence in prostate cancer. World J Urol 2005;23:1–9.
38. Schweizer MT, Gulati R, Mostaghel EA, Nelson PS, Montgomery RB, Yu EY, et al. Docetaxel-related toxicity in metastatic hormone-sensitive and metastatic castration-resistant prostate cancer. Med Oncol 2016;33:77.
39. Bahl A, Masson S, Malik Z, Birtle AJ, Sundar S, Jones RJ, et al. Final quality of life and safety data for patients with metastatic castration-resistant prostate cancer treated with cabazitaxel in the UK Early Access Programme (EAP) (NCT01254279). BJU Int 2015;116:880–7.
40. Chesire DR, Dunn TA, Ewing CM, Luo J, Isaacs WB. Identification of aryl hydrocarbon receptor as a putative Wnt/beta-catenin pathway target gene in prostate cancer cells. Cancer Res 2004;64:2523–33.
41. Lal J, Asthana OP, Nityanand S, Gupta RC. Pharmacokinetics of centchroman in healthy female subjects after oral administration. Contraception 1995;52:297–300.
42. Flores ML, Castilla C, Gasca J, Medina R, Perez-Valderrama B, Romero F, et al. Loss of PKCdelta induces prostate cancer resistance to paclitaxel through activation of Wnt/beta-Catenin pathway and Mcl-1 accumulation. Mol Cancer Ther 2016;15:1713–25.
43. Petre-Draviam CE, Cook SL, Burd CJ, Marshall TW, Wetherill YB, Knudsen KE. Specificity of cyclin D1 for androgen receptor regulation. Cancer Res 2003;63:4903–13.
44. Trosset JY, Dalvit C, Knapp S, Fasolini M, Veronesi M, Mantegani S, et al. Inhibition of protein-protein interactions: the discovery of druglike beta-catenin inhibitors by combining virtual and biophysical screening. Proteins 2006;64:60–7.
45. Bhat RV, Shanley J, Correll MP, Fieles WE, Keith RA, Scott CW, et al. Regulation and localization of tyrosine216 phosphorylation of glycogen synthase kinase-3beta in cellular and animal models of neuronal degeneration. Proc Natl Acad Sci U S A 2000;97:11074–9.
46. Zhang N, Jiang Y, Zou J, Yu Q, Zhao W. Structural basis for the complete loss of GSK3beta catalytic activity due to R96 mutation investigated by molecular dynamics study. Proteins 2009;75:671–81.
47. Ikeda S, Kishida M, Matsuura Y, Usui H, Kikuchi A. GSK-3beta-dependent phosphorylation of adenomatous polyposis coli gene product can be modulated by beta-catenin and protein phosphatase 2A complexed with Axin. Oncogene 2000;19:537–45.
48. Gao D, Vahdat LT, Wong S, Chang JC, Mittal V. Microenvironmental regulation of epithelial-mesenchymal transitions in cancer. Cancer Res 2012;72:4883–9.
49. Figiel S, Vasseur C, Bruyere F, Rozet F, Maheo K, Fromont G. Clinical significance of epithelial-mesenchymal transition (EMT) markers in prostate cancer. Human Pathol 2016;61:26–32.
50. Wang M, Ren D, Guo W, Huang S, Wang Z, Li Q, et al. N-cadherin promotes epithelial-mesenchymal transition and cancer stem cell-like traits via ErbB signaling in prostate cancer cells. Int J Oncol 2016;48:595–606.

51. Hadler-Olsen E, Winberg JO, Uhlin-Hansen L. Matrix metalloproteinases in cancer: their value as diagnostic and prognostic markers and therapeutic targets. Tumour Biol 2013;34:2041–51.
52. Hanahan D, Weinberg RA. Hallmarks of cancer: the next generation. Cell 2011;144:646–74.
53. McDonald ER, El-Deiry WS 3rd. Cell cycle control as a basis for cancer drug development (Review). Int J Oncol 2000;16:871–86.
54. Lu Y, Wei C, Xi Z. Curcumin suppresses proliferation and invasion in non-small cell lung cancer by modulation of MTA1-mediated Wnt/beta-catenin pathway. In Vitro Cell Dev Biol Animal 2014;50:840–50.
55. Rao Y, Wang H, Fan L, Chen G. Silencing MTA1 by RNAi reverses adhesion, migration and invasiveness of cervical cancer cells (SiHa) via altered expression of p53, and E-cadherin/beta-catenin complex. J Huazhong Univ Sci Technolog Med Sci 2011;31:1–9.